Proceedings of 2022 IEEE
International Conference on Mechatronics and Automation
August 7 - 10, Guilin, China

Inter-subject Variability Evaluation of Continuous Elbow Angle from sEMG using BPNN

He Li , Shuxiang Guo *, Dongdong Bu , Hanze Wang

Key Laboratory of Convergence Biomedical Engineering System and Healthcare Technology,
The Ministry of Industry and Information Technology, School of Life Science,
Beijing Institute of Technology, Haidian District, Beijing 100081, China
* Corresponding author: guoshuxiang@bit.edu.cn

***Abstract*—As a non-invasive approach, surface electromyographic (sEMG) signal has great potential for application in human-robot interfaces, such as the upper-limb exoskeleton rehabilitation device. However, due to the differences in activity level of muscles, there exists high inter-subject variability. In this work, the influence of inter-subject variability for elbow continuous motion is evaluated through a shallow neural network (BPNN), and user-dependent and user-independent models are established respectively. In user-dependent model, training and testing sets are from the same subject, new set of the same person as during training is used as the input of network. The user-independent models are constructed by the same user and another additional user to determine inter-subject variability in model construction. To evaluate the degree of inter-subject variability, evaluation criteria and statistical method are adopted. Through the prediction results, and further the value of evaluation criteria and the plot of statistical method, it can be seen that the inter-subject variability on sEMG has a huge impact on the regression of elbow continuous angle, which can provide reference for the future study of building sEMG generalized modeling to estimate elbow angles.**

***Index Terms*—surface electromyographic (sEMG), inter-subject variability, joint continuous motion, neural network**

I. INTRODUCTION

Stroke is an acute cerebrovascular disease, which is stroke is the second-leading cause of death and the third-leading cause of death and disability combined in the world. 20% of stroke patients fully recover from physical and mental impairment, 60% suffer from impairment of motor, language, sensory and cognitive systems, and the remaining 20% die in [1]. Hemiplegia is a condition caused by a stroke-related neurological deficit that reduces sensory and motor abilities on one side of the body. It has been found that 80% of stroke survivors suffer from hemiplegia. The main consequence of this disorder is usually weakness or inability to exercise on one side of the body. Upper extremity hemiparesis is the most common post-stroke disability[2], leading to significant difficulty when carrying out their activities of daily living (ADL).

Rehabilitation training is an effective method to improve the physical function for stroke patients with upper limb hemiparesis [3]. Robot-assisted therapy of upper limbs has become a safe and feasible assisted rehabilitation therapy after stroke [4]. Over the last years, robot-assisted rehabilitation devices have been designed to provide intensive and repetitive robot-assisted rehabilitation[5][6], which can bring advantages over traditional rehabilitation techniques [7].

For Upper-limb robot-assisted therapy, the design of Human-Robot Interfaces (HRIs) is vital [8]. The intention-based recognition controls the device to facilitate the execution of movements. Different approaches based on invasive and non-invasive approaches have been proposed to design HRIs in recent years. Invasive methods implant electrodes directly into the brain or other electrically excitable tissue to record signals from the peripheral or central nervous system or muscle, this kind of methods have high resolution and accuracy[9]. Non-invasive methods include the follows: electroencephalography (EEG) [10], electrooculography (EOG) [11], brain-machine interfaces [12 13], surface electromyography (sEMG) [14][15] and so on. sEMG a stable non-invasive approach, which has been successfully adopted for controlling robotic-assisted prostheses and rehabilitation exoskeleton devices due to its inherent intuitiveness and effectiveness [16]. Compared with EEG signals, sEMG signals are easy to obtain and process, and can provide effective information about the movement a subject. However, due to differences in the muscle activity levels[17][18], there exist high inter-subject variability, which limits the use of sEMG.

In this paper, we focused on the evaluation of inter-subject variability and its influence on the regression of continuous elbow motion. Based on the inter-subject variability regarding sEMG, its impact on continuous motion estimation of the elbow joint in rehabilitation is further evaluated. Myo armband is used as the sEMG acquisition device, and the signals after preprocessing and feature extraction are used as the input of Back Propagation Neural Networks (BPNN), then user-dependent and user-independent models are established respectively. Further quantitative analysis is performed by the evaluation criteria of MSE and MAE, and statistical analysis is performed through Bland-Altman. The experimental results demonstrate that inter-subject variability makes the elbow joint motion estimation with a large error, which should be considered in the future for building generalized model (independent of subject) used in the prediction of the joint motion angle.

The rest of the paper is organized as follows. The experimental protocol and processing methods are illustrated in Section II. In Section III, the results and discussion are reported. Finally, the conclusion is presented in Section IV.

978-1-6654-0853-0/22/$31.00 ©2022 IEEE

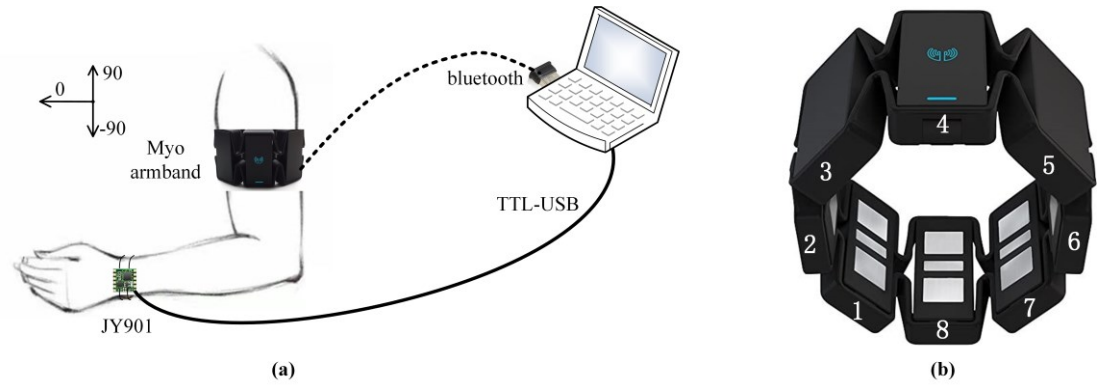

(a) (b)

Fig. 1 (a) The experimental setup used for collecting sEMG signals (b) MYO armband showing the sensor sequences.

II. Material and Methods

In this section, we describe the characteristics of the experimental device, the processing process of sEMG, the modeling process using BPNN and the evaluation criteria respectively.

A. Experimental protocol

In this study, six healthy participant (4 male and 2 females) age ranging from 20 to 30 years old (mean = 23.7 years; standard deviation [SD] = 1.4 years) are selected. All the participants have no musculoskeletal disorders at the time of experiments. Before the test, each participant is introduced the experimental protocol and signed the informed consent. The upper and forearm should be kept as relaxed as possible to avoid muscle tension which could introduce offsets to the signal. Furthermore, the wrist of subject should be kept along with the forearm, ensuring that the elbow joint moves in only one degree of freedom (DOF) in the vertical plane. The experiment is repeated six times for each subject, with a one-minute rest between adjacent experiments to avoid muscle fatigue. During the sEMG acquisition process, the upper arm naturally hangs down, the forearm starts from the natural drooping state, moves around the elbow joint, and returns to the natural drooping state after one minute of motion.

The upper limb's sEMG data of each subject is acquired using a wearable armband sensor (Myo armband, as shown in Fig. 1) developed by Thalmic Labs Inc, which is a commercially available device that includes 8 equidistance sEMG sensors [19]. The acquisition diagram of sEMG and angle is shown in Fig. 1b. The MYO armband is placed at the same location of each subject's forearm like that the fourth sensor is in line with the middle finger of hand. With the help of a custom — written script via Bluetooth communication, the sEMG data-unitless 8-bit unsigned integer values are sampled at 200 Hz and directly streamed to the Matlab's (MATLAB 2020b, MathWorks) workspace, the sEMG data results from a proprietary conversion algorithm from mV. Then the raw sEMG can be assessed through the Myo software development kit (SDK). An angle sensor (JY901, WIT motion) is attached on the forearm, the angle obtaining through it as the target value, and the sampling frequencies of angle sensors is set to 20 Hz.

B. Data preprocessing and feature extract

sEMG signal is a kind of weak and easily interfered bioelectrical signal. The inherent noise in equipment and inherent non-stationarity of signal can both degrade the quality of the acquired signal, so the data preprocessing step is indispensable to obtain high-quality signals. The acquired sEMG data has been normalized to [-1 1] through MYO SDK, then are high-pass filtered at 20 Hz (4^{th}-order Butterworth high-pass filter, shown in Fig. 2a) to remove DC offsets and the noises in the low-frequency range, and notch filtered at 50 Hz (1^{th}-order Butterworth band-stop filter, shown in Fig. 2b)

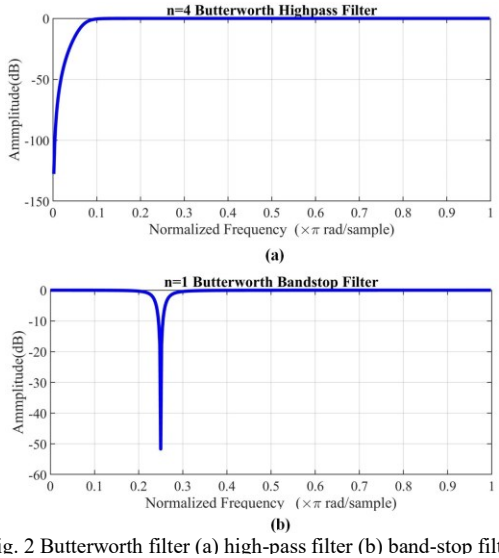

Fig. 2 Butterworth filter (a) high-pass filter (b) band-stop filter

to avoid power-frequency interference.

After filtering, considering that sEMG signals are highly non-stationary, so the sliding window method is used to segment the sEMG signal to facilitate the analysis of signals with high frequencies. Through sliding window method, the raw sEMG signal will be divided into separate windows. Due to the real-time characteristics of Human-Robot Interfaces (HRIs), the total time of segment length and processing time of generating estimation control commands should not exceed 300 ms [20]. At the same time, the window segmentation length should not be too short, because with the decrease of

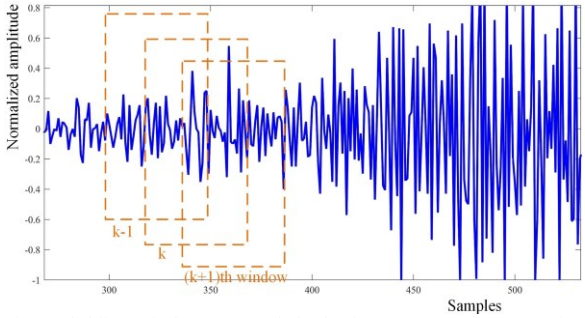

Fig. 3 Slidding window approach for basic measurements extraction illustrated for the case of the sEMG signal.

the window segmentation length, the deviation and variance will increase, which will reduce the availability of the system. In order to introduce more samples, fixed-size overlapping sliding window (FOSW) method is used. That is, the sliding stride is smaller than the window size, resulting in two adjacent segments overlapping with each other. In this study, a shifting analysis window with a time length of 250ms (50 sample points) and an increment of 100 ms (150 ms overlapping) is used to segment the sEMG signals into a series of analysis windows (as shown in Fig. 3). And to make sure that sampling points of sEMG are consistent with that of the elbow joint angles obtained by the angle sensor, the angles are also divided into separate windows with a time length of 25ms (5 sample points) and an increment of 10 ms (15 ms overlapping).

Further, to estimate the angle of joint motion, different features should be extracted from each separate window to construct feature vector. The feature vector can represent the original sEMG signal information, which is vital to accurate recognition. There are several methods of feature extraction, such as time domain, frequency domain, time-frequency domain, etc. Time domain information describes the signal waveform with time as a variable, and is closely associated to signal amplitude. Frequency domain features are more used to analyze the fatigue degree of muscle. Time-frequency domain features can better induce transient effects of muscular contractions. Considering that time domain features is closely associated to sEMG amplitude, which reflects the angle information. Hence, five time-domain simple features including Mean Absolute Value (as (1) shows), Zero Crossings(as (2) shows), Slope Sign Changes (as (3) shows), Root mean square(as (4) shows), and Integrated Absolute Value (as (5) shows) are used in our study.

Mean Absolute Value (MAV)

It is evaluated by taking the average of each signal within an analysis window, defined as:

$$MAV = \frac{1}{N}\sum_{k=1}^{N} | x_k | \tag{1}$$

where N is the number of samples in a separate window, x_k represents the kth sample within an analysis window.

Zero Crossings (ZC)

It represents the number of times signal x_k crosses zero within an analysis window; it is a simple measure associated with the frequency of the signal. The ZC count increased by one if:

$$\{| x_k - x_{k-1} | > 10e-7\} \&\& \{x_k * x_{k-1} < 0\} \tag{2}$$

Slope Sign Changes (SSC)

It is related to signal frequency and is defined as the number of times that the slope of the sEMG waveform changes sign within an analysis window. The SSC count increased by one if:

$$\begin{aligned} &\{(x_k - x_{k-1})(x_k - x_{k+1}) > 0\} \\ &and \{| x_k - x_{k-1} | > 10e-7 or | x_k - x_{k+1} | > 10e-7\} \end{aligned} \tag{3}$$

Root mean square (RMS)

It refers to the effective value of muscle discharge within an analysis window, and its change depends on the change of sEMG amplitude, defined as:

$$RMS = \sqrt{\frac{1}{N}\sum_{k=1}^{N} x_k^2} \tag{4}$$

Integrated Absolute Value (IAV)

It represents the sum of the absolute values of signal amplitude in a separate analysis window, defined as:

$$IAV = \sum_{k=1}^{N} | x_k | \tag{5}$$

Based on the analysis window with a time length of 250ms and an increment of 100 ms (150 ms overlapping), sEMG activation curve can be obtained through extracting from each window the following features: MAV、ZC、SSC、RMS、IAV.

C. Continuous joint motion estimation based on BPNN

After getting the features for all subjects, angle learning and estimation implemented through machine learning is the next step that need to be realized. In this paper, BPNN is used for angle regression and prediction, which is one of the well-known algorithms in neural networks. The network consists of three layers: input layer, hidden layer and output layer, where the hidden layer transmits important information between the input layer and the output layer. The process of BP neural network is mainly divided into: (1) signal forward propagation; (2) error back propagation. According to the gradient descent method, the loss function is continuously reduced, so that the network can get closer and closer to the real relationship. The model of BPNN is shown in Fig. 4, which includes the neuronal structure and the network structure.

The feature sequences form the input data X of BPNN and the joint angle Y is the output signal. In this study, we suppose that

$$\begin{cases} X = [x_1, ..., x_i, ...x_8] & i = 1:8 \\ x_i = [MAV_i, ZC_i, SSC_i, RMS_i, IAV_i] & \\ Y = [y_1, ..., y_k, ...x_N] & k = 1:N \end{cases} \tag{6}$$

Where i represents the ith channel of MYO armband, k represents the kth point of the output, and N is the total number of the point of the output.

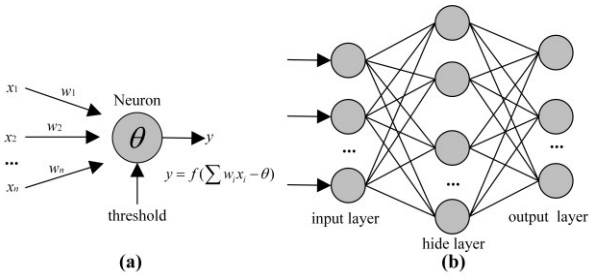

Fig. 4 BPNN (a) Neuronal structure (b) network structure

The Levenberg-Marquardt algorithm is adopted as the training algorithm. Although the algorithm occupies a larger amount of memory, it takes less time. When generalization stops improving, training stops automatically, as indicated by an increase in the mean squared error of validation sample. Through the neural network, estimated angle of elbow motion can be calculated, but the obtained angle curve in not smooth. Further, the output of neural network is filtered using an 8-point sliding window. After sliding window filtering, a smooth angle sequence can be obtained, which can further used in HRIs through sEMG.

D. *Evaluation criteria*

In this paper, the mean square error (MSE), Regression value (R), mean angle error (MAE) and Bland-Altman (B&A) statistical analysis is introduced to evaluate the performance of estimation. MSE and R is the evaluation parameter during modeling. MSE is the average squared error between the estimated angles and the target angles, shown in (7). The lower the value of MSE, the better the estimation effect. R measure the correlation between the estimated angles and the target angle. The higher the value, the better the estimation effect. MAE is the average error between output angles and target angles, shown in (8). The lower the value of MAE, the better the estimation effect. The B&A plot analysis is adopted to evaluate the bias between the estimated and the target angles.

$$MSE = \sum_{i=1}^{N} (\bar{y}_i - y_i)^2 \tag{7}$$

$$MAE = \frac{1}{N} \sum_{i=1}^{N} (\bar{y}_i - y_i) \tag{8}$$

Where y_i is the actual joint angle at ith data point and $\bar{y}_i$ represents the estimated angle at ith data point, and N is the total number of data points.

III. Results and Discussion

In this section, we present and discuss the model obtained with BPNN. To verify the effect of inter-subject variability during continuous motion of elbow, the prediction comparison of user-dependent and user-independent model is provided. Finally, we present the results of the evaluation using indicators.

A. *The performance of Modeling*

For each subject (A-F), the first five sets of data are used for modeling, and the last one set of each subject is as the additional test. Samples are randomly divided into training set, validation and test set, the ratio is 70%:15%:15%. Training R, validation R, and test R are recorded during the training process (TABLE I). The MSE and R of additional test are the evaluation of angle estimation effect (TABLE I). Across all the subjects, the training R are all greater than 95%, the R of additional test are also greater than 95%, and the MSE all less than 250.

Taking subject A as an example, the regression figure of is shown in Fig. 5. Fig. 5(a) is the regression value during training, Fig. 5(b) is the regression value of additional test

TABLE I THE ESTIMATED PERFORMANCE OF BPNN MODEL FOR EACH SUBJECT

subject	Training R	Validation R	Test R	Additional test	
				MSE	*R*
A	0.9634	0.9631	0.9575	222.5428	0.9627
B	0.9753	0.9655	0.9588	228.8031	0.9567
C	0.9725	0.9490	0.9503	245.1478	0.9572
D	0.9766	0.9483	0.9575	239.5296	0.9507
E	0.9731	0.9716	0.9723	131.4279	0.9713
F	0.9738	0.9561	0.9530	249.1167	0.9540

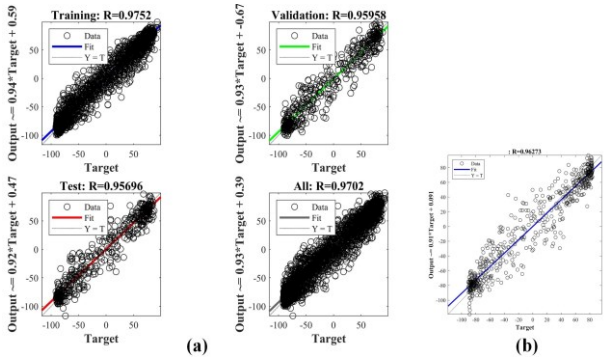

Fig. 5 The regression of BPNN model (a) the regression value during training (b) the regression value of additional test

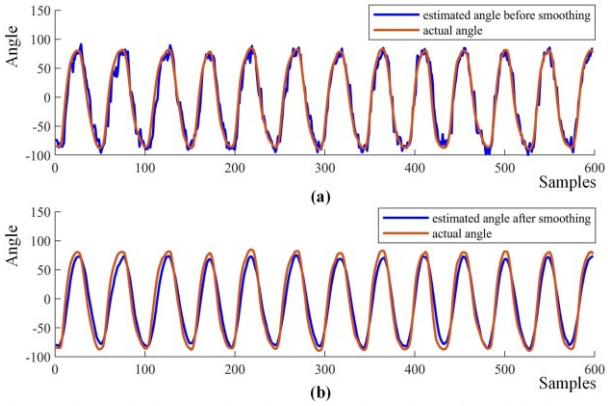

Fig. 6 The prediction results of angle (a) the estimated angle before and after smoothing (b) comparison of estimated angle and actual angle

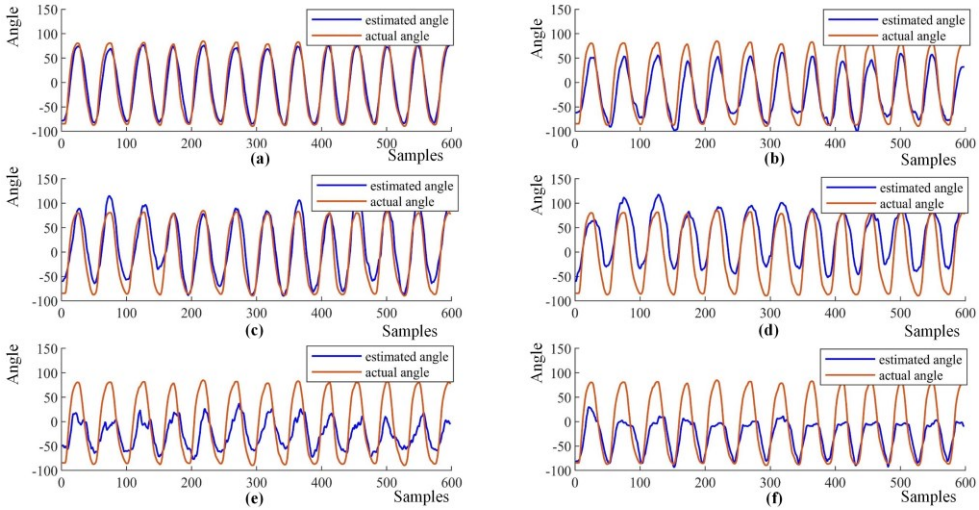

Fig. 7 Estimation comparison of user-dependent and user-independent model. (a) estimated angle of subject A using its own model, (b) estimated angle of subject A using the model of subject B, (c) estimated angle of subject A using the model of subject C, (d) estimated angle of subject A using the model of subject D, (e) estimated angle of subject A using the model of subject E (f) estimated angle of subject A using the model of subject F

TABLE II ESTIMATED ANGLE EVALUATION OF SUBJECT A FOR USER-DEPENDENT AND USER-INDEPENDENT MODEL

Criteria	Model of A	Model of B	Model of C	Model of D	Model of E	Model of F
MSE	222.5428	895.8131	727.0325	2.4547e+03	2.4756e+03	2.2192e+03
MAE	12.3478	24.0627	22.2568	40.5557	42.1468	37.9354

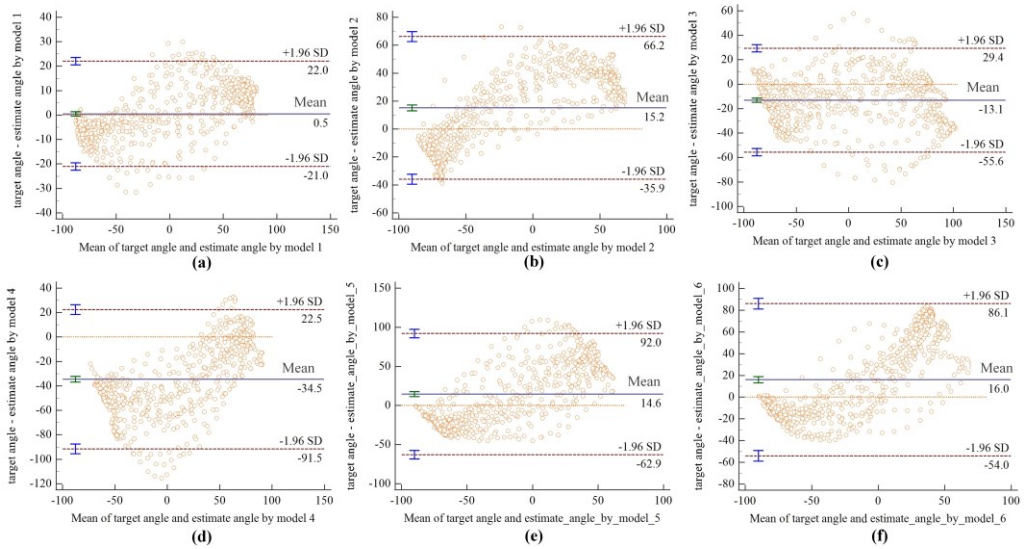

Fig. 8 The Bland-Altman plots of estimated angle and the actual angle. (a) the estimated results of A#6 using model A (b) the estimated results of A#6 using model B (c) the estimated results of A#6 using model C (d) the estimated results of A#6 using model D (e) the estimated results of A#6 using model E (f) the estimated results of A#6 using model F

(A#6 representing the sixth time experiment of subject A). The prediction results can be seen from Fig. 5 intuitively which compared the motion tracking of estimated and target angle. And through the comparison before and after sliding window filtering (Fig. 6), it can be found that the filtering effect is very obvious, and the filtered output can be further used in HRIs.

B. The performance of Modeling Estimation result of user-dependent and user-independent model

In the above section, the BPNN models (built with the first five sets) for each subject have been established. In this section, the inter-subject variability will be illustrated using user-dependent and user-independent model.

Plan A (user-dependent): For the user-specific, individual models are trained and evaluated for each of the users using their own data. That is, the model established by each user's own first five sets of data are used to predict the user's new data (the sixth set of data).

Plan B (user-independent): Select one user as the existing subject, and the remaining users take turns as new subjects.

That is, the model *i*th subject is used to predict the angle of the *j*th subject ($i \neq j$).

Take the first subject (subject A) as an example, the estimated result of angle using its own model is shown is Fig. 7(a), and Fig. 7(b-f) are the estimated results of angle using model of subject B, C, D, E, F respectively. As can be seen from Fig. 7(a), when estimation of joint motion angle for a specific subject, well prediction result can be obtained by using its own model. However, if the data used for modeling is not from the same subject as the prediction process, there exist a large error compared to the target value, as shown in Fig. 7(b-f).

C. *Evaluation based on inter-subject variability*

Through the above, intuitive observation can be made. Next, specific indicators and statistical methods will be used for further evaluation. In order to evaluate the prediction accuracy, MSE and MAE are employed in this study which can reflect the error and relationship between the prediction results and actual angle.

TABLE II record the evaluation results of MSE and MAE criteria of subject A, using model of subject A-F respectively, and Fig. 8 plot the corresponding B&A. As can be seen from TABLE II and Fig. 8, only the prediction angle corresponding to model A (that is, the training sEMG data and test sEMG data are from the same subject) shows satisfactory prediction effects. That is, the model trained by samples of specific users always perform badly when it is applied to another. The reason of the poor detection result is due to the inter-subject variability on sEMG. This paper only evaluates the inter-subject variability, and does not consider the intra-subject variability. In future research, we will further consider both the inter-subject variability and the intra-subject variability.

IV. CONCLUSION

In this paper, evaluating the effect of inter-subject variability on continuous elbow motion is the focus. Through the comparison of prediction results of user-dependent model and user-independent model, it can be found that the estimated angles using user-independent model have a poor detection result. It can even be said that a model that established using the sEMG data of a specific subject is almost inapplicable to another subject, which provide reference for the future research on the generalized model for elbow angle estimation. In order to improve the generalizability of the model, it is necessary to reduce or remove the impact of inter-subject variability. On the one hand, data augmentation is needed. On the other hand, the research on combining transfer learning will be further considered, such as using domain adaptation to map different individual features into a common space to improve model adaptability.

REFERENCES

[1] Feigin JVL, Brainin M, Norrving B et al., "World Stroke Organization (WSO): Global Stroke Fact Sheet 2022," International Journal of Stroke, vol. 17, no. 1, pp. 18-29, 2022.

[2] Hatem SM, Geoffroy S, Margau DF et al., "Rehabilitation of Motor Function after Stroke: A Multiple Systematic Review Focused on Techniques to Stimulate Upper Extremity Recovery," Frontiers in Human Neuroscience, vol. 10, 2016.

[3] Liu Y, Guo SX, Yang ZY et al., "A Home-based Bilateral Rehabilitation System with sEMG-based Real-time Variable Stiffness", IEEE Journal of Biomedical and Health Informatics, vol.25, no.5, pp.1529-1541, 2020.

[4] Veerbeek JM, Langbroek-Amersfoort AC, van Wegen EE, "Meskers CG, Kwakkel G. Effects of robot-assisted therapy for the upper limb after stroke: a systematic review and meta-analysis," Neurorehabil Neural Repair, vol. 31, no. 2, pp. 107–121, 2017.

[5] Gopura R, Bandara D, Kiguchi K et al., "Developments in hardware systems of active upper-limb exoskeleton robots: A review," Robotics and Autonomous Systems, vol. 75, pp. 203–220, 2016.

[6] Lauretti C, Cordella F, Guglielmelli E et al., "Learning by Demonstration for planning activities of daily living in rehabilitation and assistive robotics," IEEE Robotics and Automation Letters, vol. 2, no. 2, pp. 1375–1382, 2017.

[7] Calabrò RS, Cacciola A, Bertè F et al., "Robotic gait rehabilitation and substitution devices in neurological disorders: where are we now?," Neurological Sciences, vol. 37, no. 4, pp. 503–514, 2016 .

[8] Rodgers H, Bosomworth H, Krebs H I et al., "Robot-assisted training compared with an enhanced upper limb therapy programme and with usual care for upper limb functional limitation after stroke: the RATULS three-group RCT," Health technology assessment (Winchester, England), vol. 24, no. 54, pp. 1-232, 2020.

[9] Waldert S. "Invasive vs. non-invasive neuronal signals for brain-machine interfaces: will one prevail?," Frontiers in Neuroscience, vol. 10, pp. 1–4, 2016.

[10] Belfatto A, Scano A, Chiavenna A et al., "A Multiparameter Approach to Evaluate Post-Stroke Patients: An Application on Robotic Rehabilitation," Applied Sciences, vol. 8, no. 11, 2248, 2018.

[11] Huang Q, Chen Y, Zhang Z et al., An EOG-based wheelchair robotic arm system for assisting patients with severe spinal cord injuries," Journal of Neural Engineering, vol. 16, no. 2, 2019.

[12] Soekadar SR, Witkowski M, Gómez C et al., "Hybrid EEG/EOG-based brain/neural hand exoskeleton restores fully independent daily living activities after quadriplegia," Science Robotics, vol. 1, no. 1, eaag3296, 2016.

[13] Crea S, Nann M, Trigili E, Cordella F, Baldoni A, Badesa FJ, et al. "Feasibility and safety of shared EEG/EOG and vision-guided autonomous whole-arm exoskeleton control to perform activities of daily living," Scientific Reports, vol. 8, 10823, 2018.

[14] Yang ZY, Guo SX, Liu Y, Hirata H, Tamiya T, "An Intention-based Online Bilateral Training System for Upper Limb Motor Rehabilitation", Microsystem Technologies, Vol.27, No.1, pp.211-222, 2021.

[15] Bu DD, Guo SX, Li H, "sEMG-based Motion Recognition of Upper Limb Rehabilitation Using the Improved Yolo-4 Algorithm", Life 2022, vol.12, no.1.

[16] Farina D, Jiang N, Rehbaum H et al., "The extraction of neural information from the surface EMG for the control of upper-limb prostheses: emerging avenues and challenges," IEEE Transactions on Neural Systems and Rehabilitation Engineering. vol. 22, pp. 797–809, 2014.

[17] Singh R, Chatterji S, "Trends and challenges in EMG based control scheme of exoskeleton robots-a review," International Journal of Scientific and Engineering Research, vol. 3, pp. 1–8, 2012.

[18] Rechy-Ramirez EJ, Hu H. "Bio-signal based control in assistive robots: a survey," Digit Communication Networks. vol. 1, no. 2, pp. 85–101, 2015.

[19] Thalmic Labs. 2013. Available: https://www.myo.com/. (Accessed 1November 2017).

[20] Gao B, Wei C, Ma H et al., "Real-Time Evaluation of the Signal Processing of sEMG Used in Limb Exoskeleton Rehabilitation System," Applied Bionics and Biomechanics, vol. 2018, no.6, pp. 1-7.